

# Singing sands, musical grains and booming sand dunes

A. J. PATITSAS

*Department of Physics and Astronomy, Laurentian University, Sudbury, ON, Canada, P3E 2C6*

*e-mail address: tpatitsas@sympatico.ca,  
Tel.: 705 525 4098; Fax: 705 675 4868.*

The final version of this paper was published in the Journal of Physical and Natural Sciences, Volume 2, Issue 1, 2008. It is available on line with the above title.

**Abstract**– The origin of the acoustic emissions from a bed of musical grains, impacted by a pestle, is sought in a boundary layer at the leading front of the pestle. The frequencies of the shear modes of vibration in such a layer are compared with the observed frequencies. It is assumed that such a layer is the result of the fluidization of the grain asperities due to the high stress level at the front end. Such a boundary layer can also account for the emissions from plates of sand sliding on a dune surface and from grains shaken in a jar.

*Keywords:* Singing sands; musical grains; booming dunes; acoustic emissions

## 1. INTRODUCTION

Acoustic emissions occur when singing beach sands are stepped on or impacted in a dish by a pestle, with dominant frequency,  $f_d$ , in the range from about 250 to 2500 Hz (Takahara [1], Nishiyama and Mori [2], Miwa et al. [3], Haff [4], Qu et al. [5], Sholtz et al. [6], Nori et al. [7], Brown et al. [8]). The emitted sound has musical quality, especially with  $f_d$  under about 1000 Hz, hence the terms; singing, musical, and sonorous sands. When nearly spherical glass beads are placed in a dish and impacted by a pestle, they present little resistance to the motion of the pestle and there is no acoustic emission. However, when such beads, 0.18 mm in diameter, were placed in a dish, 5 cm in diameter, and impacted by a pestle, 4.3 cm in diameter, an acoustic emission described as, "a shrill unpleasant note" was recorded having a wide frequency spectrum peaking at about 3000 Hz (Brown et al. [8]). Furthermore, when silent grains, such as common salt, were squeezed by a pestle 12 mm in diameter in a plastic cell 20 mm in diameter, an acoustic emission was evoked with dominant frequency somewhat above 1000 Hz (Patitsas [9]). When sand grains, from the dunes in the Kalahari Desert, South Africa, were heated in an oven at 200  $C^o$  for half hour and then placed in a glass jar, 1/2 full, a strong emission (roar) occurred upon a rapid tilt of the jar (Lewis [10]). Furthermore, by rotating the jar about a horizontal axis along its length, at about 120 revolutions per minute, a continuous roar was obtained. When grains from the booming dunes of Sand Mountain, NEV., USA, were placed in a glass jar, about 1/3 full and shaken back and forth, an acoustic emission occurred with  $f_d \approx 280$  Hz (Leach and Rubin [11]). However, no sound was emitted when the same grains were placed in a large dish, several cm in depth, and impacted by a pestle. In a natural avalanche at Sand Mountain,  $f_d$  is about 66 Hz (Nori et al. [7]). In the report by Grambo [12], there is reference to wind-blown singing sand grains at the Basin Head Beach in Prince Edward Island, Canada. In a private communication, the author described the sound as a high pitched whistle, when the grains are blown across the beach by strong winds. Furthermore, a similar account can be found in the book by Courzon [13], regarding the sand dunes at Jebel Nakus (Hill of the Bell) in the Peninsula of Sinai on the eastern shore of the Red Sea.

Silica gel grains, used for humidity control purposes and characterized by non-spherical geometry and by extreme surface angularity, resist the motion of the pestle and emit a low frequency pleasant note when impacted by a pestle. Reference to resistance to shear in musical grain beds can be found in the report by Sholtz et al. [6]. All grains become somewhat musical, the silent less so, when placed in a dish with depth of only about 1 cm and impacted by a rod, about 2 cm in diameter. Glass beads, 0.6 mm in diameter, become musical in such an arrangement, as can be seen in Fig. 6 in the report by Nishiyama and Mori [2]. Therefore, we proceed to classify certain grains as singing or musical, if a pleasant sound is emitted when the grains are placed in a large dish, to a depth of several cm, and impacted lightly by a rod about 2 cm in diameter. The signals observed on an oscilloscope screen, corresponding to the acoustic emissions from repeated impactions, are not identical and at times they differ appreciably, especially after the grain bed is shaken about. The values of the dominant frequency,  $f_d$ , can vary by as much as  $\pm 15\%$  between successive impacts. We think that this is mainly due to the history dependence of the geometric configuration of the void and arching distributions in the grain bed.

As far back as 1889, regarding the booming dunes, it was assumed by Bolton [14] that, "the sounds result from thin films of soluble impurities deposited on the grains". Furthermore, in the book by Bagnold [15] we read as follows, "Hence it seems that the disturbance speed which will set a given sand in vibration is determined by some unknown property of the grains themselves-some property, it is most likely, of their molecular surface structure". In the report by Qu et al. [5], it is argued that honeycomb-like pits on the surface of the quartz grains could play a role towards their musicality. Goldsack et al. [16] used infrared (IR) spectroscopy to study the chemical composition of the molecular layer on the surface of musical grains and they suggest that the relevant absorption bands could be due to clusters

of water in an amorphous silica layer. However, such a layer cannot be viewed as an added impurity, since grains regain their musicality after prolonged milling and washing (Nishiyama and Mori [2], Miwa et al. [3]). In the case of the silica gel grains, it is suggested that the existence of a surface layer of the same composition as the core but of different density, presumably due to the presence of water, is responsible for the musicality of the grains (Kilkeny et al. [17]). Therefore, it is fairly safe to argue that the singability (musicality) of a grain mass is determined by the physical state of the grain surface. In the report by Sholtz et al. [6], there is an account of the various suggestions, or hypotheses, as to the cause of such acoustic emissions. However, no sufficient attention has been devoted to the principal physical observable, *i. e.*, the Energy Density Spectrum, or the Frequency Spectrum for brevity, of the acoustic emissions. In a recent report by Patitsas [9], there was an attempt to account for such spectra, based on compression standing wave patterns in the shear zones or slip channels in the impacted grain bed.

## 2. EXPERIMENTAL RESULTS AND CONCEPT DEVELOPMENT

### 2.1 Asperity fluidization and the slip channel

Figure. 1 depicts the only known radiograph of the motion of sonorous and silent sand grains, in a large dish, impacted by a plunger with speed of penetration somewhat above 30 cm/s. According to the report by Miwa et al. [3], the acoustic emission occurs concurrently with the slip layers. In the report by Patitsas [9], the slip layers are referred to as the slip channels, or otherwise known as the shear zones, or shear bands.

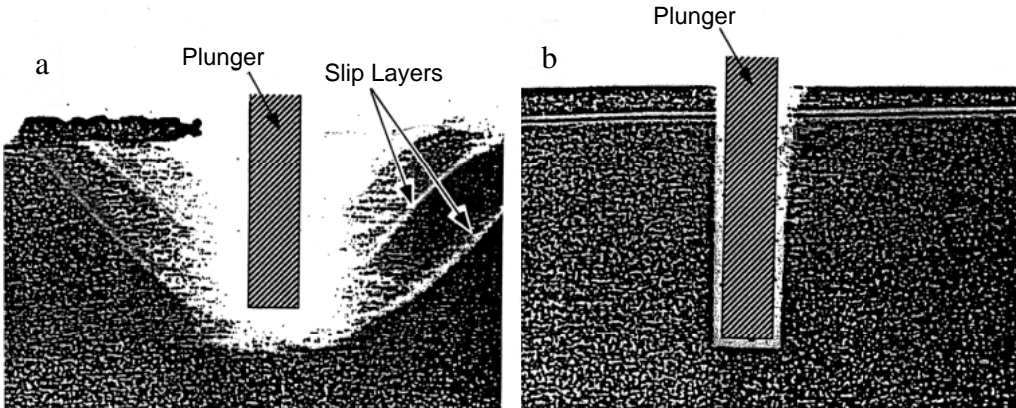
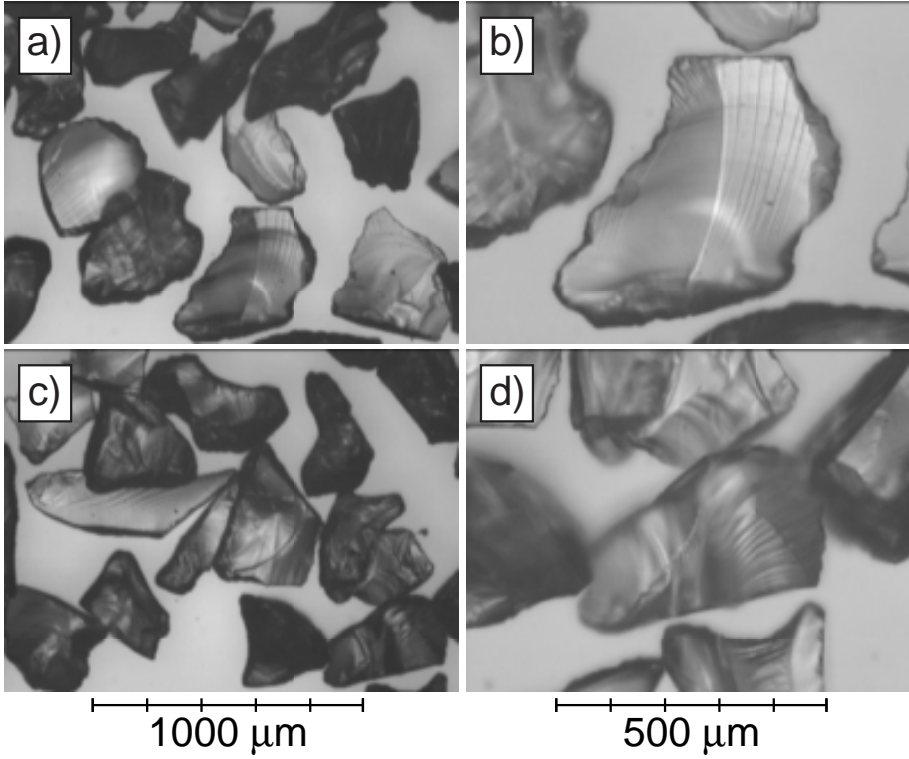


Fig. 1. X-ray radiographs depicting a rectangular steel plunger, 3 cm wide by 5 cm deep, impacting a bed of (a) musical sand and (b) silent sand. (a) the slip channels (shear zones) were labeled as, Slip Layers, by Miwa et al. [3]. (b) silent sand has no slip channels. Reproduced by permission of the principal author.

Evidence of the existence of such a slip channel was observed by the following procedure: an ordinary paint mixing wood stick, 30 mm wide by 4.4 mm thick, tapered to a sharper edge in the last 3 mm, was used to impact manually the silica gel grains seen in Fig. 2. The grains were placed in a glass jar, 9 cm in diameter by 14 cm in height, filled to the height of 6 cm. After a few impacts, with the stick slanted a few degrees from the vertical direction, a small crater was formed and a strip of grains, about 2 mm wide and parallel to the plane of the stick, could be seen emerging simultaneously with the acoustic emission. The distance of the strip from the tapered side of the stick was about 15 mm and the angle between the plane of the stick and the line from the tapered end to the strip was about  $40^\circ$ .

Fig. 2. Photographs of silica gel grains, utilized in this report, obtained by optical microscopy. Part (c) depicts better than part (a) the lack of roundness of the grains. Parts

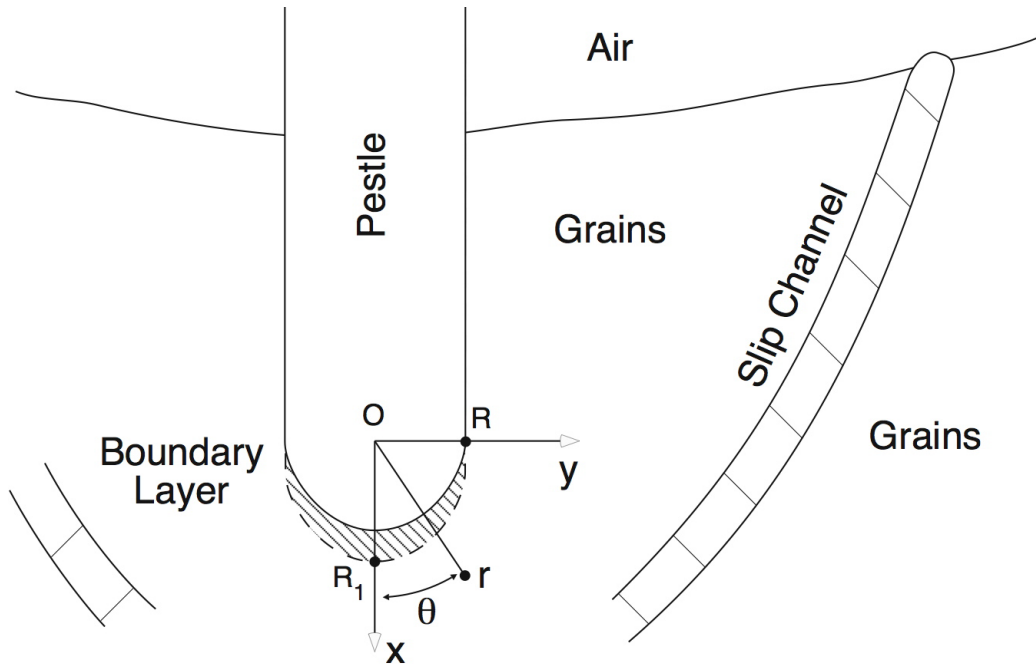


(b) and (d) are magnifications of parts (a) and (c) in order to depict the ridge formations. Average diameter,  $\bar{d} \approx 0.4$  mm.

Figure 3 depicts a schematic of the paint stick geometry, but in the more conventional form, where the bottom of the pestle is rounded and is driven vertically into the grain bed. The grains are assumed to flow into the boundary layer at around  $\theta = 0^\circ$  and exit at around  $\theta = 60^\circ$ .

Fig. 3. Schematic of a vertical cross-section of a descending rectangular pestle of width  $2R$  rounded at the bottom with radius  $R$ . The pestle dimension,  $L$ , along  $\hat{z}$ , is assumed to be considerably larger than  $R$ .  $R_1 = R + b$ , *i.e.*, the boundary layer has thickness  $b$ . The pestle could also be a rounded circular rod of radius  $R$ .

The jar was kept closed and in a dark environment for nearly two years, since grains were removed for the recording of the signals seen in Figs. 4 and 5. At that time, the musicality of the grains was at a higher level and a light touch of the surface, by some pestle, could result in a pleasant note. The signal in Fig. 4 was obtained by the light touch of the silica gel grains placed in a small plastic cell, 3 cm in diameter by 3 cm in height. It is estimated that the small rounded end of the brass pestle, 8.5 mm in diameter, penetrated the grain bed by about 10 mm in 0.1 s, implying an average velocity of penetration equal to about 10 cm/s. One could argue that the contact of the pestle with the grains lasted for only a fraction of the duration of the signal in Fig. 4, resulting in higher penetration velocity. However, that would imply a resonance-like vibration in the entire grain bed, resulting in a signal with large initial amplitude and decaying with time, contrary to the inserts in Figs. 4 and 5. Furthermore, the dominant frequency,  $f_d$ , would decrease with increased bed size, contrary to the frequency spectrum shown in Fig. 5, where the mortar size is considerably larger than that of the plastic cell. Since the signal ceased to exist when the pestle came to rest, it can be concluded that the grain bed was viscous. The frequency spectrum in Fig.



6 depicts a noticeable frequency content at around 2000 Hz, and the insert depicts the frequency spectrum of the signal emitted when (silent) local beach sand grains were impacted by the small end of the brass pestle in the same porcelain mortar. The frequency content around 2250 Hz is deemed to be due to the incoherent grain-grain collisions around the pestle.

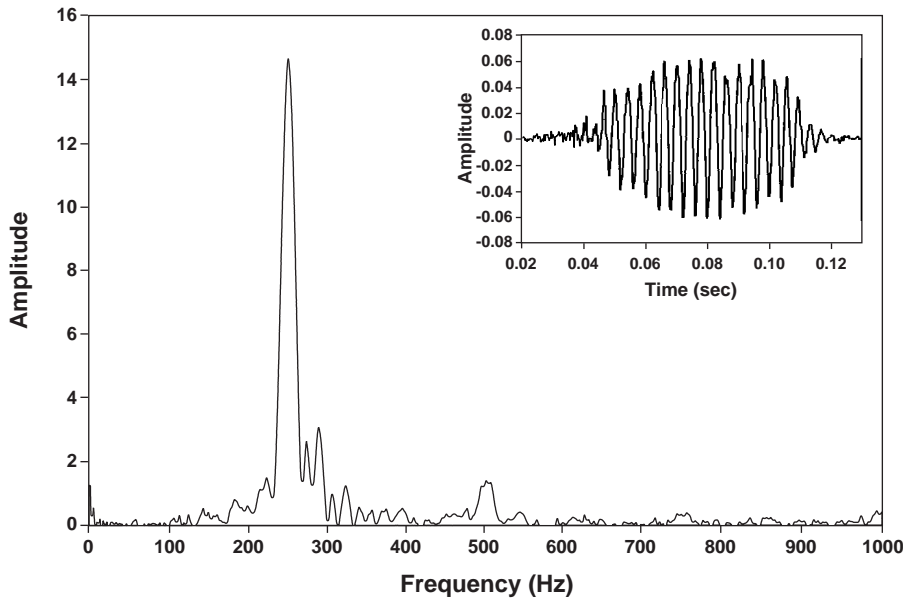


Fig. 4. Energy density spectrum (frequency spectrum) of the signal shown in the insert. The microphone recorded signal was emitted when the small rounded end of a brass pestle, 8.5 mm in diameter, impacted the silica gel grains in a small plastic cell, 3 cm in diameter by 3 cm in height. Depth of penetration was about 10 mm. Dominant frequency,  $f_d \approx 252$  Hz.

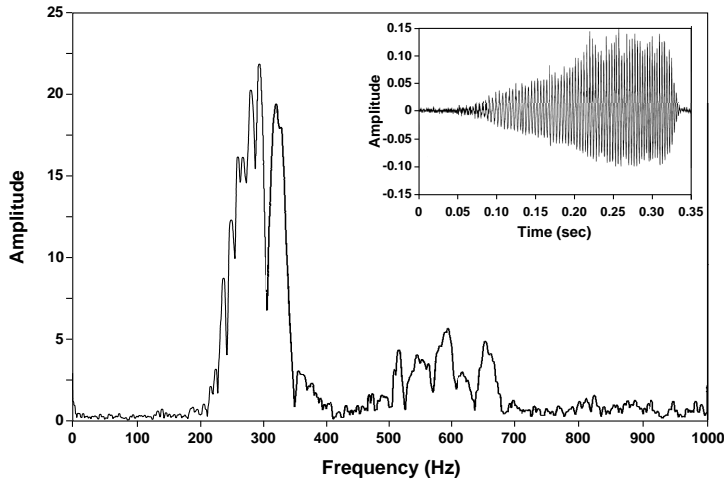


Fig. 5. Same as in Fig. 4, but the grains were impacted, with more force in a porcelain mortar, 5.5 cm in diameter by 5 cm in height. Depth of penetration was about 2 cm and  $f_d \approx 297$  Hz.

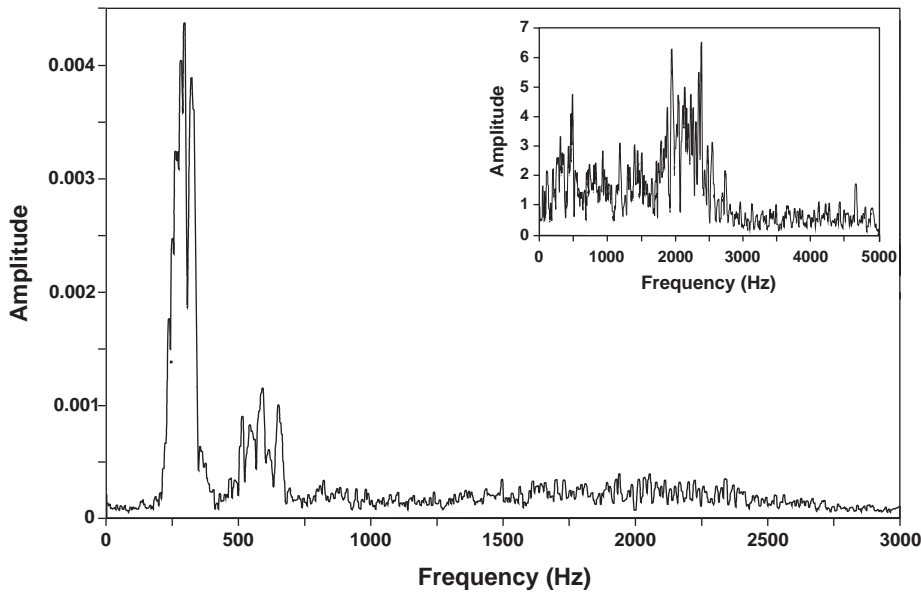
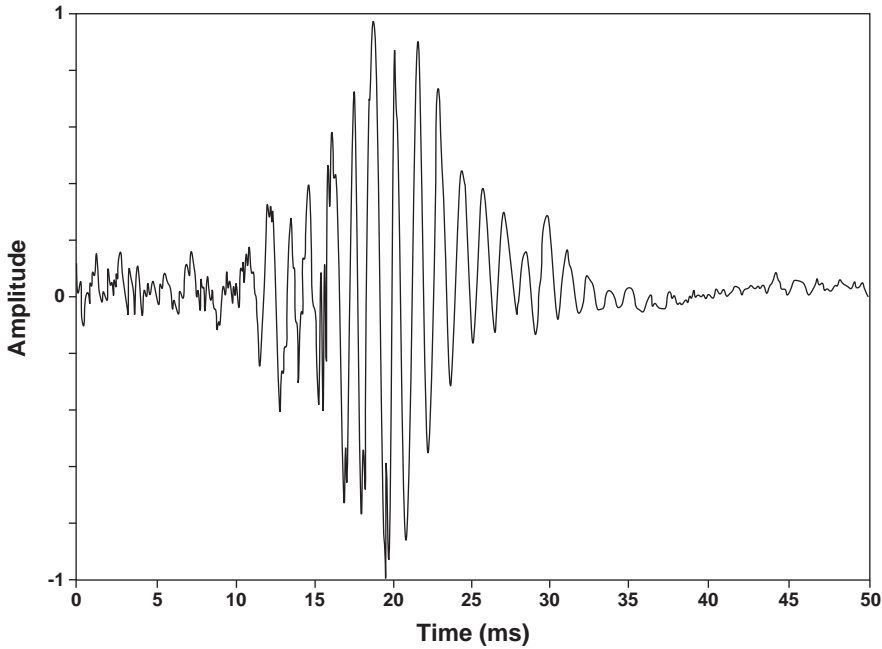


Fig. 6. Same as in Fig. 5, but extended to 3000 Hz in order to show the frequency content around 2000 Hz due to the incoherent grain-grain collisions. Insert: Frequency spectrum of the hissing-like sound from silent sand grains,  $\hat{d} \approx 0.3$  mm, when impacted by the small end of the brass pestle in the porcelain mortar. The signal is not shown.

Fig. 7. A microphone recorded signal from silent local beach sand grains impacted by the eraser end of a regular pencil with diameter  $D = 7$  mm. The grains were placed in a porcelain cup with flat bottom and diameter  $D = 9$  cm. Sand depth,  $H \approx 1$  cm,  $f_d \approx 700$  Hz. When  $H$  was about 5 cm, the signal was noise-like.

Figure 7 depicts the signal emitted when the same silent sand grains were impacted sharply by the rubber end of a regular pencil in a large porcelain coffee cup with flat bottom



and with sand depth,  $H$ , of only about 1 cm. The signal is of short duration, but it has the distinct dominant frequency,  $f_d \approx 700$  Hz. Figure 8 depicts the signal emitted when Kotobikihama sand, from the Kyoto prefecture, Japan, was impacted in the same cup with a wood rod,  $D = 25$  mm, in a sand depth  $H \approx 7$  cm in part (a), and  $H \approx 1$  cm in part (b). In part (a), we observe the emergence of a lower frequency,  $f_d \approx 500$  Hz, in the last few ms. In part (b), the signal is considerably more monochromatic, with  $f_d \approx 700$  Hz. The effect of the rigidity of the cup floor on the musicality of the grains is more evident in Fig. 9, where Ottawa sand was used in the same cup. The signal in part (a) can be considered as noise-like. In order to examine the effect of the rigidity and of the surface texture of the floor, a circular cloth piece, cut from a wash towel, was inserted at the bottom of the cup and then silica gel grains or other musical sand grains were poured on top to the depth of about 1 cm. There was no acoustic emission when the grains were impacted with the 25 mm wood rod. Only a faint emission was produced when the cloth was replaced by a plastic piece cut from an ordinary yogurt container cap. The importance of the rigidity of the medium around the leading front of the pestle can be seen in the experimental reports by Takahara [1], Brown et al. [8] and Patitsas [9], where normally silent grains placed in a cylindrical vessel produced a somewhat musical sound, when impacted by a rod with diameter slightly smaller than that of the vessel.

Fig. 8. Same as in Fig. 7, but with Kotobikihama sand grains in the same cup impacted with a wood rod,  $D = 25$  mm. (a):  $H \approx 7$  cm.  $f_d \approx 1200$  Hz during the first 30 ms, then,  $f_d \approx 500$  Hz during the last 20 ms. (b):  $H \approx 1$  cm,  $f_d \approx 700$  Hz.

The most efficient approach, in generating the acoustic emissions, was to hold the rod vertically with one hand, the bottom touching the grain surface, and then to tap or to push the top of the rod with the other hand. The depth of penetration could thus be controlled to vary from about 2 cm to 5 cm. It was observed that  $f_d$  was nearly the same when the rods were allowed to free fall from a certain height, as when tapped into the grain bed, implying that the mass of the tapping hand was not an important factor in the determination of the frequency,  $f_d$ . However, the signal in the former case was of shorter duration and not as well-defined. More discussion in this regard can be found at the end of Section  $A_1$ .

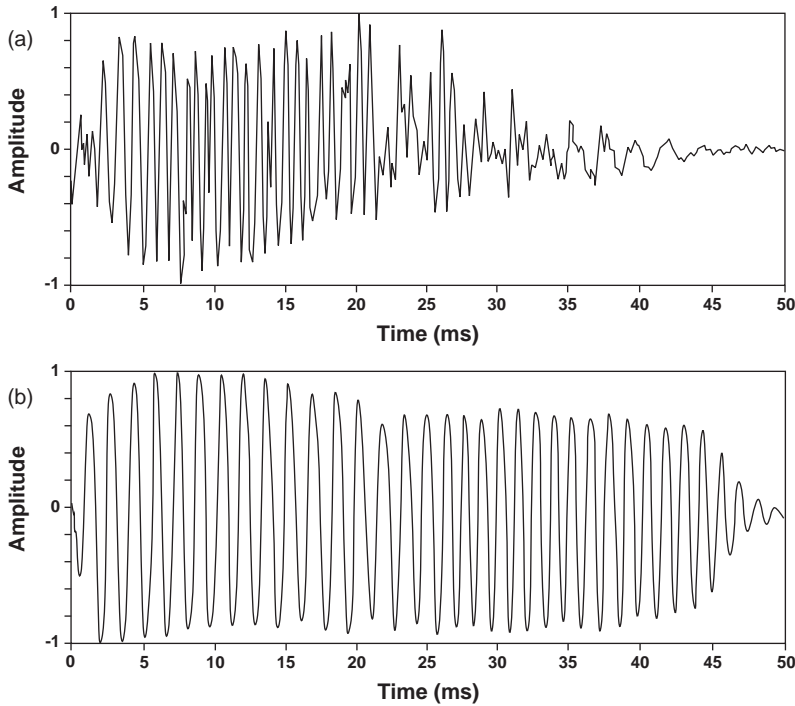
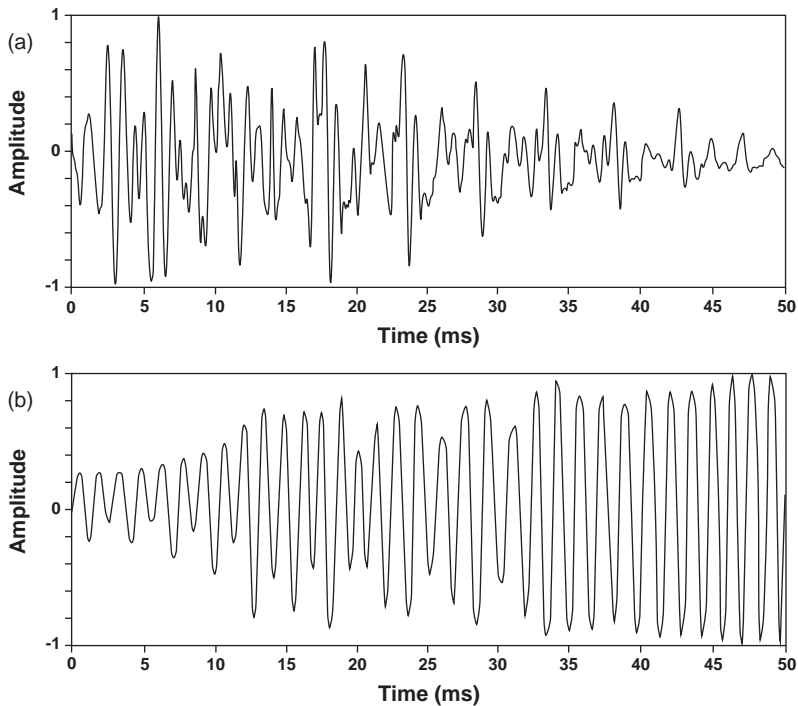


Fig. 9. Same as in Fig. 8, but with Ottawa sand. (a):  $H \approx 7$  cm, signal is noise-like, (b):  $H \approx 1$  cm,  $f_d \approx 700$  Hz.

On the basis of the experimental evidence presented above, it can be argued that the grain mass, around the impacting pestle, is in a quasi-gaseous and possibly turbulent kinematical state, in the case of the silent grains. Effectively, the grains acquire sufficient kinetic energy to move past one another with relative ease, *i. e.*, the grains interact with each other primarily during collisions, which last only for a few  $\mu$ s. In what follows,  $\bar{d}$ ,  $\bar{v}$  and  $s$  are the average grain diameter, the average grain random velocity and the average inter granular separation distance respectively. Then the collision rate between two grains can be roughly estimated from the relation,  $r_c = 1/2(\bar{v}/s) = 1/(2\bar{d})(\bar{d}/s)\bar{v} = 1875$  Hz, for  $\bar{d} = 0.4$  mm,  $\bar{d}/s = 30$  and  $\bar{v} = 5$  cm/s. Therefore, the frequency content around 2000 Hz in the insert in Fig. 6, which is perceived as a hissing sound, can be attributed to such a random collision rate. Considerable frequency content at around 6000 Hz, in other cases involving sand grains, can be attributed to larger values of  $\bar{d}/s$ . However, a large part of the hissing sound has to originate with the direct contact, rubbing and colliding, of the grains with the pestle surface.

Fig. 10. Microphone recorded signal when Kotobikihama sand grains were impacted by a wood rod,  $D = 16$  mm, in the porcelain cup. Sand depth,  $H \approx 5$  cm,  $f_d \approx 1050$  Hz.

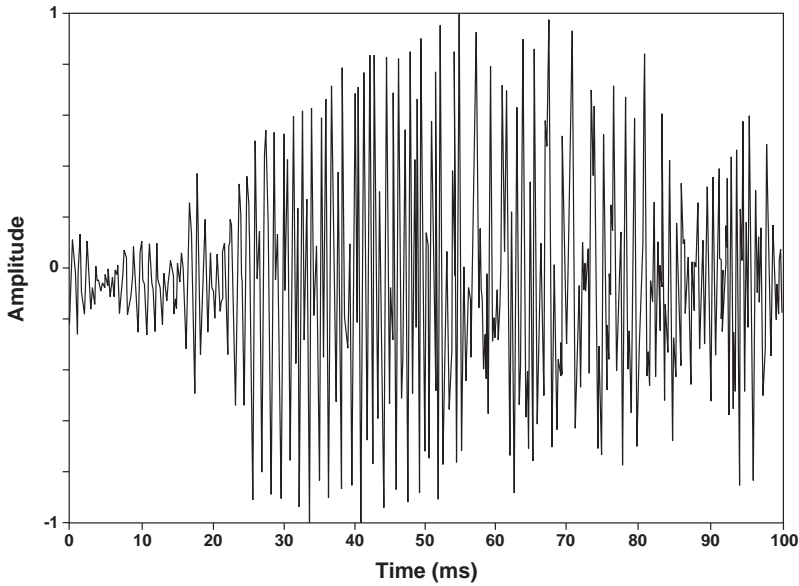
In the case of the musical grains, such flowability appears to be impossible due to surface conditions, which are not yet well understood. It is possible that, in the static configuration, there is a kind of interlocking between the grain asperities that results in a relatively high degree of rigidity. Then, the high rigidity results in the build-up of the stress level in the entire grain bed, until ruptures (slip channels) occur at the regions of weakness, as the pestle penetrates into the grain bed (Fig. 1a). In such regions, there is a precipitous decrease in the modulus of rigidity and the slip channels tend to act like roller boards for the overburden to slide towards the surface. This is an economical way of displacing the grain mass towards the surface in view of the interlocking between the grain asperities in the regions outside the slip channels.



We assume that the grain mass, in a slip channel, is in a state of a viscoelastic liquid with sufficient viscosity to support a shear wave with phase velocity,  $c_s$ , on the order of a few m/s, while the compression phase velocity,  $c_p$ , is considerably higher. In the context of this hypothesis, when sufficient energy is delivered to the channel by the pestle, the stresses acting on the grain contact points, combined with the relative motion between the grains, result in the liquidization (fluidization) of the grain asperities at the contact points. Such a fluidization could be the result of the heat generated locally and or the result of the generation of  $\mu\text{m}$  size sub-grains, which act as ball bearings between two hard surfaces. Such an assumption is consistent with the colloidal nature of silica gel, where the gel consists primarily of silicon dioxide sub-micron colloidal particles. Such fluidization results in the precipitous reduction in the value of the modulus of rigidity of the asperities and in the precipitous reduction in the shear phase velocity in the grain mass. In the report by Qu et al. [5], it is suggested that the pits on the singing grains could contribute to their singability, and in Fig. 2, we observe ridges on the surface of some grains, suggesting the presence of large asperities. When the viscosity,  $\eta$ , becomes very large so that the fluid begins to behave like a solid,  $\eta$  can be estimated from (31.1) in the book by Landau and Lifshitz [18], i. e.,  $\eta \approx \tau\mu$ , where  $\tau$  is the relaxation time and  $\mu$  is the Lamé' constant, or the modulus of rigidity, defined in (2) in the Appendix. Then, with mass density,  $\rho = 1500 \text{ kg m}^{-3}$ ,  $c_s = 2 \text{ m/s}$  and  $\tau \approx 1/f_d$ ,  $f_d = 250 \text{ Hz}$ ,  $\eta$  is on the order of  $24 \text{ kg/(ms)}$ , i. e., 24000 times that of water at  $20^\circ\text{C}$ . In the book by Joseph [19], it is stated that some liquids can display rigidity when the viscosity is larger than a critical value and in Table F. 1., in the same source, we read that for honey,  $c_s = 13.5 \text{ m/s}$ , while for 50 % aqueous Glycerol,  $c_s = 0.047 \text{ m/s}$ .

## 2.2 Asperity fluidization and the boundary layer

The radiograph shown in Fig. 1a implies that the slip channels do not move downwards with the pestle, but that new channels are generated as the pestle penetrates deeper into the grain bed. If the acoustic emission were due to the slip channel closest to the end of the pestle, then, when it is replaced by the most recent farther below, a discontinuation in the emission would be inevitable,. However, Figs. 8a and 10 suggest otherwise, i. e., that the geometry of



the source of the acoustic emission remains fairly stable during the pestle penetration. Such a stable source has to be sought in a boundary layer around the leading front of the pestle, as depicted in Fig. 3. The vibration takes place, principally, in the central part, where the thickness,  $b$ , can be assumed to be constant. In such a boundary layer, the stress level is highest, thus providing for the excitation of the modes of vibration in such a layer. However, the presence of the slip channel(s) is critical in regulating the stress level around the pestle so that a well-defined layer can be realized. In order to establish that the boundary layer is limited to the leading front surface of the pestle, a 16 mm hole was drilled at the bottom of a plastic container, 6.2×6.2 cm in size. A long wood rod of the same diameter was passed through the hole and musical grains were poured into the container to a height of about 10 cm. The rod could be moved up and down with relative ease without an acoustic emission, apart from a low level hissing sound.

In order to better understand the conditions that lead to the formation of the boundary layer, we may visualize the grain mass in the container to move upwards with the velocity,  $V_p$ , towards the stationary pestle having cross-sectional area  $S$ . The grains, lying a few mm away from the bottom of the pestle, experience intense shear and compression stresses as they are forced to change direction of motion by nearly  $90^\circ$ . Such stresses lead to the liquidization of the grain asperities at the contact points and this in turn leads to the drastic reduction in the modulus of rigidity. The boundary layer is treated as a continuum, and the grains vibrate according to the particle motion dictated by the given shear mode of vibration in the boundary layer. In order for the stress level, around the bottom of the pestle, to rise to a sufficient level to bring about the formation of the boundary layer, the grain mass as a whole must be characterized by a level of rigidity not found in a silent grain mass. The grains in the boundary layer remain in close contact as they slide past one another. In this sense, the determining factor for musicality is the physical state of the grain asperities, while shape and roundness are nearly irrelevant (Fig. 2).

When a grain bed in the large cup,  $H \approx 1$  cm, was impacted by the larger rods,  $D \geq 25$  mm, it was observed that  $H$  was reduced to about 5 mm after the impact, suggesting that the boundary layer thickness,  $b$ , was about 5 mm. On the basis of the above observation, we may argue that in the case of Fig. 8b, where  $f_d \approx 700$  Hz, the boundary layer thickness,  $b$ , was on the order of 5 mm. In the case of Fig. 8a,  $f_d \approx 1200$  Hz and thus, it can be concluded that either  $b$  was smaller than 5 mm and or the phase velocity,  $c_s$ , was higher than in the case of Fig. 8b, the latter being the more plausible. However, the important conclusion is that only a small part of the grain column below the pestle was responsible for the acoustic emission

when  $H \approx 7$  cm. Effectively, if the entire column was responsible for the acoustic emission, then,  $f_d$  in Fig. 8a ought to be appreciably lower than in Fig. 8b. In order to examine the effect of the surface texture of the large cup,  $D \approx 9$  cm, on the acoustic emissions, a pouch was formed from a flexible plastic net-like mesh used to wrap items for decorative purposes. The pouch was then placed inside the cup and the silica gel grains were poured inside to the depth of about 5 cm. The mesh openings were small enough so that the grains could not pass through. It was determined that the acoustic emissions were not affected perceptibly by such a pouch.

In the first part of the Appendix,  $A_1$ , we show that the frequencies of vibration, generated by the pestle-grain interaction, cannot be specified in terms of propagating waves, but rather in terms of standing wave patterns or standing modes of vibration. In the second part  $A_2$ , we examine the modes of vibration when the pestle bottom is the flat end of a rectangular plunger with dimensions  $L$  and  $2R$  along  $\hat{z}$  and  $\hat{y}$  respectively (Fig. 3). In part  $A_3$ , we examine the case when the pestle is the same as in part  $A_2$ , but the bottom is rounded as shown in Fig. 3. In part  $A_4$ , we examine the case when the pestle bottom is the rounded end of a rod of radius  $R$ , and in part  $A_5$ , when the pestle bottom is the flat end of a rod of radius  $R$ .

In part  $A_2$ , we argue that the frequencies corresponding to the shear modes of vibration in the boundary layer of thickness,  $b$ , are given by the rather familiar transcendental equation (8). The lower root,  $r_1 = \alpha_1 b$ , corresponds to the vibration of a loaded short spring, when the load factor,  $L_f \rightarrow \infty$ . The corresponding wave number is,  $k_{s1} \approx \alpha_1$  and thus, the corresponding lower frequency is,  $f_1 = \omega/(2\pi) = c_s k_{s1}/(2\pi) = c_s/(2\pi)(r_1/b)$ . The lower root lies in the range,  $0 < r_1 < \pi/2$ , and tends to zero as  $L_f \rightarrow \infty$ . Similarly, the second frequency is,  $f_2 = c_s/(2\pi)(r_2/b)$ , where the root  $r_2$  lies in the range,  $\pi < r_2 < 3\pi/2$ . The third root lies in the range,  $2\pi < r_3 < 5\pi/2$  and so on. The plots in Fig. 11 show that the lower frequency,  $f_1$ , decreases very slowly with  $L_f$  and consequently with the pestle mass  $M$  for  $L_f < 0.1$ , and the higher frequencies decrease very slowly with  $L_f$  for all values of  $L_f$ . The plots in Fig 12 show a similar behavior even though the pestle geometry is significantly different. The frequency  $f_3$  is slightly lower than  $2f_2$ . It is thus demonstrated that the geometry of the pestle bottom is not a critical factor, i. e., the frequencies are determined principally by the thickness of the boundary layer and by the shear phase velocity,  $c_s$ , in the same layer. Such lack of dependence of the dominant frequency,  $f_d$ , on the geometry of the pestle bottom was verified by impacting the grain bed with the flat and the rounded bottom of a given rod. The near equality of  $f_d$ , measured by the microphone, when the pestle was tapped into the grain bed (Figs. 8 and 9), as when the pestle was allowed to free fall from a certain height, suggests that the microphone recorded the frequency  $f_2$ , more likely than the frequency  $f_1$ . It is the frequency  $f_2$  that varies very weakly with  $L_f$  in the entire range of  $L_f$ . There is more discussion on this point in Sections 2.3 and 2.6.

Fig. 11. Plots of the three lower frequencies,  $f_1$ ,  $f_2$ ,  $f_3$  versus the load factor  $L_f$  when the pestle is a rectangular plunger with flat bottom (Eq. 8 in the Appendix  $A_2$ ). The shear phase velocity,  $c_s$ , in the boundary layer, and the layer thickness,  $b$ , are assumed to be 5 m/s and 5 mm respectively. The Log is to the base 10.

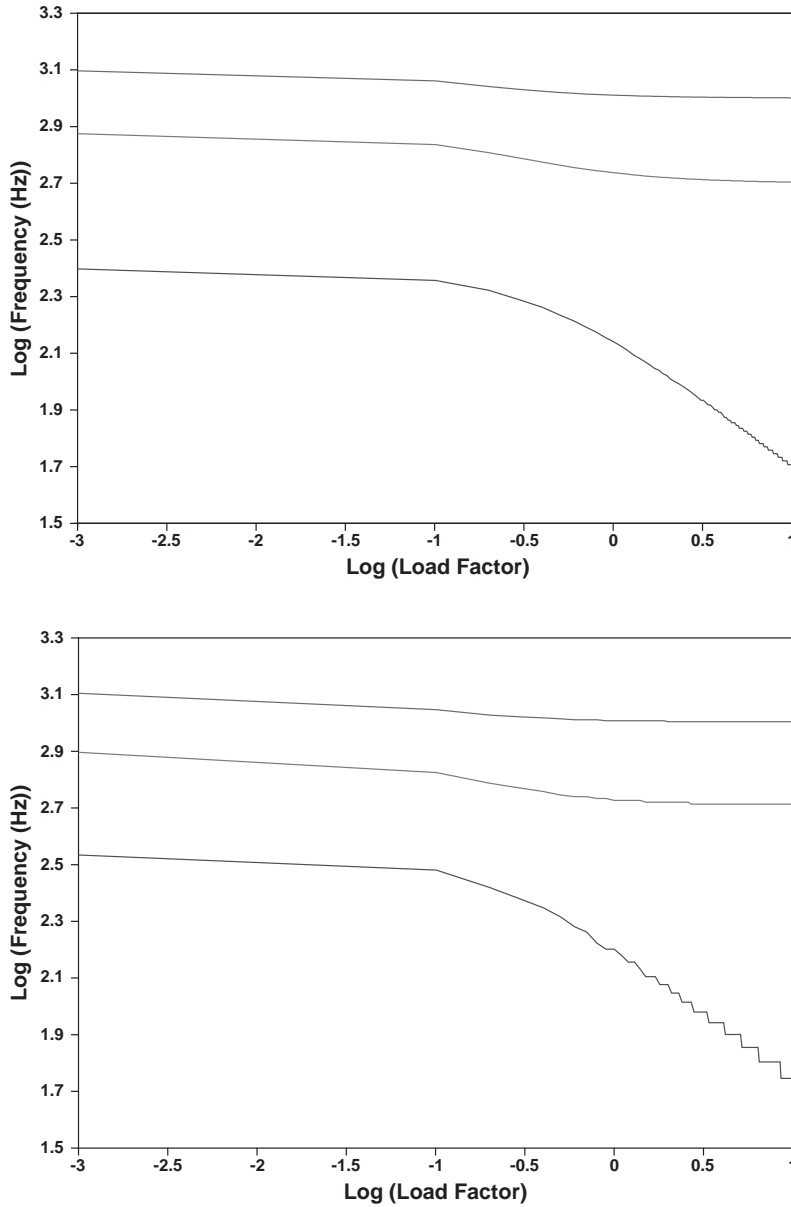


Fig. 12. Same as in Fig. 11 when the pestle is a circular rod with rounded bottom. Rod diameter,  $D = 2R = 20$  mm,  $c_s = 5$  m/s,  $b = 5$ mm, and  $\chi = 1 + b/R = 1.5$  (Eq. (18)).

It is evident, from Fig. 12, that in order for  $\text{Log}(f_1)$  to decrease somewhat linearly with  $\text{Log}(M)$ ,  $c_s/c_p$  and  $M$  must be large enough so that  $L_f > 0.1$  (18). Specifically, with  $L_f = 0.1$ ,  $M = 0.5$  kg,  $\rho = 1500$  kg/m<sup>3</sup>, and  $R = 10^{-2}$  m,  $c_s/c_p$  is equal to  $1/33$ . In Fig. 4 in the report by Nishiyama and Mori [2], it is demonstrated that the observed frequency varies approximately as  $M^{-0.5}$ . Thus, the authors concluded that the sand mass under a rod acts like a loaded short spring. However, this could be the case only when  $H \approx 1$  cm and in the limit,  $L_f \rightarrow \infty$ , as is pointed out above, regarding the signals in Fig. 8, and at the end of Section  $A_2$ . The authors used piezoelectric films (igniters) attached to the rods to record the vibration signals and the frequency of vibration. The use of such transducers is in line with the use of a geophone to record the frequency  $f_1$  in this study (Section 2.3). It is understood that in the same report, the rods were allowed to free-fall on the grain bed presumably from a height approaching zero. In the preparation of this report, it was not possible to similarly

generate strong enough signals to be detected by the geophone, seemingly due to the reduced musicality of the grains.

### 2.3 Measurement of the frequency $f_1$

Figure 13 depicts the signals emitted when the silica gel grains in the glass jar, diameter  $D = 9$  cm, were impacted with the wood rod,  $D = 16$  mm. In part (a), the signal was recorded by the microphone and has frequency  $f_d \approx 720$  Hz, which is assumed to be equal to the frequency  $f_2$ . We can observe the superimposed noise-like higher frequency content, at about 2500 Hz, due to the incoherent grain-grain collisions around the pestle and due to grain pestle collisions, as in a silent bed. In part (b), the geophone recorded only the lower frequency of 280 Hz, which we assume is equal to the lower frequency  $f_1$ .

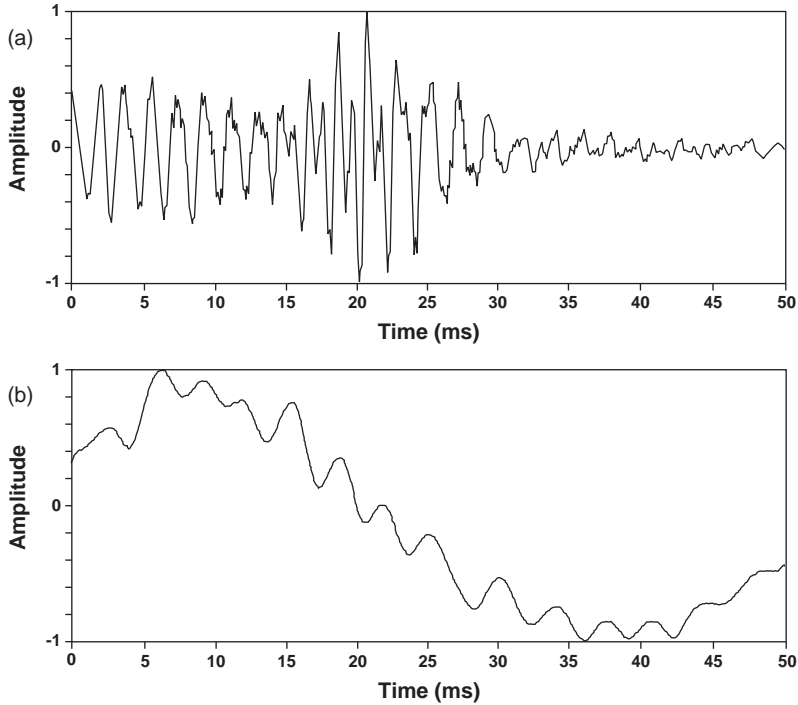
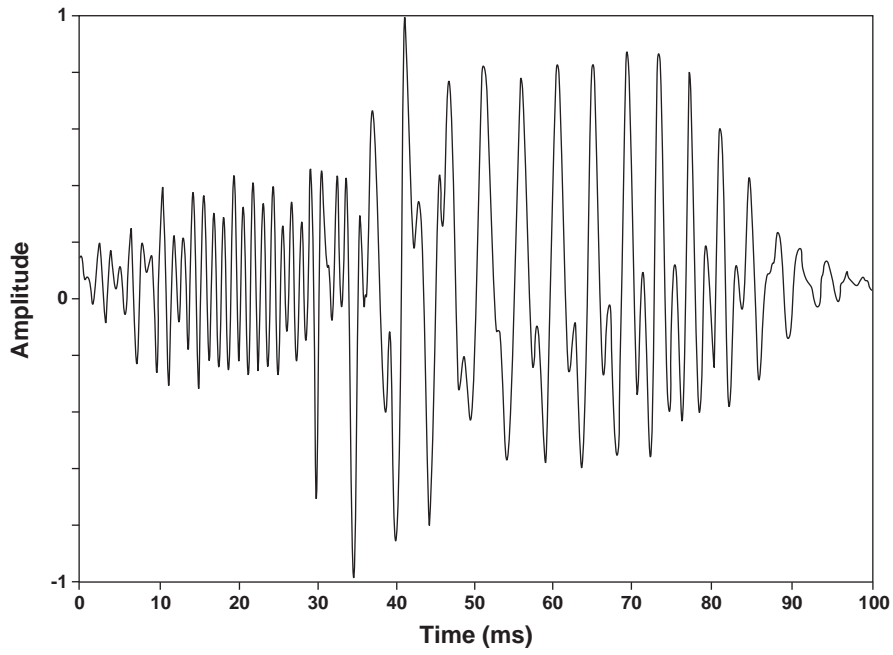


Fig. 13. Signals emitted when the silica gel grains in the glass jar,  $D = 9$  cm, grain depth  $H \approx 6$  cm, were impacted with the wood rod,  $D = 16$  mm. (a): The signal was recorded by the microphone,  $f_d \approx 720$  Hz. (b): The signal was recorded by the geophone placed on one side from the center of the jar,  $f_d \approx 280$  Hz. The slow oscillation was due to the motion of the foam pad under the jar.

The grains exhibited signs of fatigue and the bed became overly compacted after several impactions. In Fig. 14, it is shown that the same grain mass became more musical after the jar was turned about its axes. The rod penetrated the bed with less force and the higher frequency content is absent. The microphone registered the frequency,  $f_2$ , during the first 35 ms and then, it registered primarily the frequency,  $f_1 \approx 235$  Hz. During the same event, the geophone registered a nearly sinusoidal signal, not shown, with  $f_1 \approx 240$  Hz. In Fig. 15, it is demonstrated that it is possible for the geophone to detect the higher frequency  $f_2$  and in Fig. 16 it is shown that the frequencies  $f_1$  and  $f_2$  can also be recorded using sand grains with  $H \approx 1$  cm.

Fig. 14. The same as in Fig 13a, but after the jar was rotated about its axes so that the grains were rearranged. The signal was recorded by the microphone. During the first 35 ms,  $f_d = f_2 \approx 750$  Hz. Then, the major peaks are thought to correspond to  $f_1 \approx 235$  Hz. A



nearly sinusoidal signal with  $f_d \approx 240$  Hz, not shown, was also recorded by the geophone during the same event.

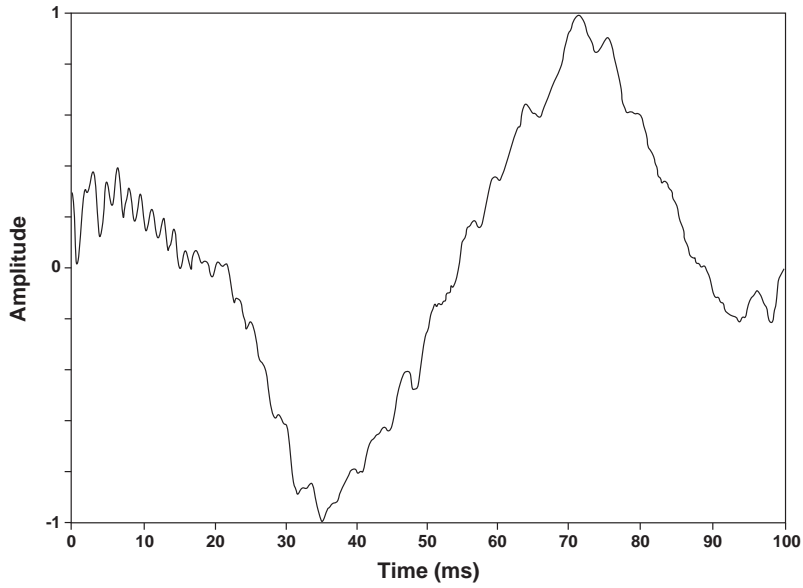


Fig. 15. The signal was recorded by the geophone when the silica gel grains, in the porcelain cup,  $H \approx 1$  cm, were impacted by the wood rod,  $D = 25$  mm. The geophone recorded the frequency,  $f_2 \approx 650$  Hz, in the first 20 ms, but then only the fundamental,  $f_1 \approx 250$  Hz.

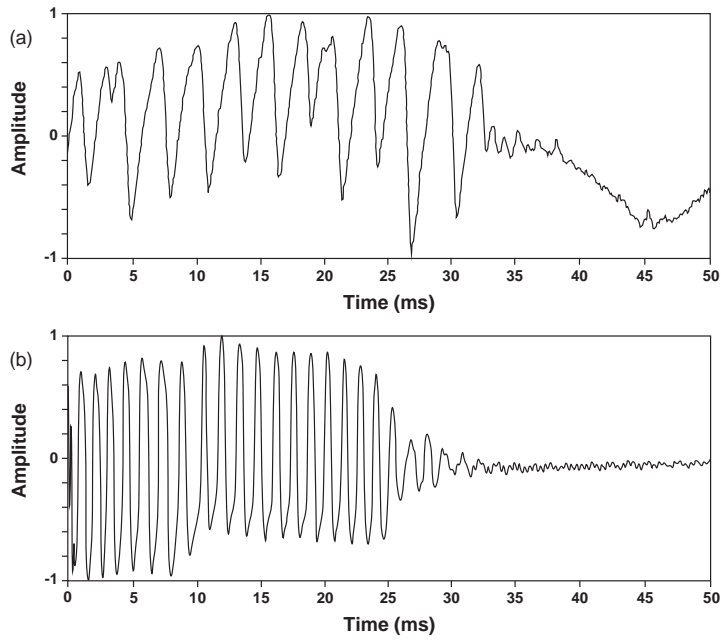


Fig. 16. Same as in Fig. 15, but with the Kotobikihama sand in the porcelain cup,  $H \approx 1$  cm. (a): The signal was recorded by the geophone,  $f_1 \approx 360$  Hz. (b): The signal was recorded by the microphone,  $f_2 \approx 760$  Hz.

It can be inferred from Fig. 8a, and from Figs. 13 to 16 that the ratio,  $f_2/f_1 \approx 2.5$  on average. From the same numerical data that led to Fig. 12, it can also be inferred that  $f_2/f_1 \approx 2.5$ , provided  $L_f < 0.1$ . For larger  $L_f$ , the ratio  $f_2/f_1$  is larger than 2.5. These results can be reconciled if we assume that the velocity ratio  $c_s/c_p$  was sufficiently low as

to render the exact value of the combined mass of the pestle and that of the hand nearly irrelevant, *i. e.*, the rods were lightly loaded.

## 2.4 Blocks of sand sliding on a sand dune

The video program by The National Geographic Society, Survivors of the Skeleton Coast Park, Namibia, Africa (1993), depicts the avalanche on the slip face of a sand dune. At first, blocks (plates) of sand, about 10 cm thick, break off and begin to slide downhill, accompanied by a low frequency sound in the neighborhood of 100 Hz. In about 5 s, the plates begin to break-up and grain avalanche on the surface becomes visible soon after. The avalanche front gradually loses thickness and comes to rest when its thickness amounts to about 3 cm, presumably at the bottom of the dune. A somewhat similar account of the avalanche evolution can be found in the reports by Haff [4] and by Sholtz et al. [6]. In the last source, it is stated that in fully developed avalanches, the sliding plates can remain intact for most of the motion and in the report by Nori et al. [7], it is stated that sliding plates of sand have the greatest acoustic output. The recent reports by Andreotti [20] and by Douady et al. [21], on the seismic and acoustic emissions due to grain flow on sand dunes, are limited to surface avalanches. In these reports, it is claimed that the dominant frequency of the seismic and acoustic emissions,  $f_d \approx 100$  Hz, is equal to the rate of collisions of a given grain with those in the layer below, as it avalanches downhill. Thus, with grain diameter  $\bar{d} = 0.2$  mm, the relative velocity between layers is,  $V_r = 2$  cm/s. Such a hypothesis implies that the 20 or so surface layers avalanching downhill are well defined. However, on p. 334 in the report by Sholtz et al. [6], there is reference to, "unusually turbulent motion, resembling a rush of water in slow motion". Towards the end of the avalanche, seen in The National Geographic video presentation, the surface grains appear to be in a kinematical state resembling that of the surface of a boiling viscous liquid. Furthermore, from observations of avalanching sand at Dumont Dunes, just south of Death Valley, California, USA, it is concluded that seismic emissions persisted after all surface grain motion appeared to have subsided (Vriend et al. [22]).

In the context of this study, the explanation of the acoustic emissions from sliding plates can be sought in (8), where a boundary layer of thickness,  $b$ , and phase velocity,  $c_s$ , is assumed to exist between the sand plate and the compacted sand mass below. Thus, with  $\alpha b = \pi$  and  $b = 10$  mm,  $k_s \approx \alpha$  is equal to 314, resulting in  $c_s = \omega/k_s = 2.0$  m/s, for  $f_2 = 100$  Hz.

It is possible that such a boundary layer continues to exist between the fixed sand mass and the mobile sand mass above, after the break-up of the plate. If that were the case, it would put an end to the nearly 150 year old mystery and controversy as to the origin of such emissions. It can be argued that the liquidization of the grain contact points occurs at some finite depth, where the stress level is sufficiently high. On p. 151 in the report by Humphries [23], regarding the booming dunes of Korizo, at the border of Libya with Chad, the author wrote; "the enormous volume of sound produced suggests that in some way a natural resonator must be involved in magnifying the sound". Then, there is reference to some 10 cm below the surface where some or all of the sound is generated. Furthermore, in the report by Andreotti [20], it is estimated that the gravitational potential energy lost per second, during an avalanche 4 m long by 1 m wide, amounts to 3 kw. Therefore, it can be inferred that the avalanche depth amounts to 9 cm, if the average grain velocity is 25 cm/s. Moreover, in the report by Douady et al. [21], it is shown that slumping sand on the dune face can result in acoustic emission with initial depth equal to 5 cm.

On p. 4969 in the report by Criswell et al. [24] the authors wrote; "Booming could also be evoked by simply pulling sand downhill with one's hand. It was necessary to keep the hand and fingers straight and to run the fingers 10-14 cm below the surface. Strong vibrations could be felt in the fingertips". The signal was recorded by a geophone at Sand Mountain and  $f_d$  was equal to 53 Hz. The signal was sufficiently intense to be heard a few m away.

Such an observation is in line with the continuous acoustic emission evoked when the 16 mm wood rod was rotated inside the 9 cm glass jar filled with silica gel grains to the depth of about 6 cm. The rod was immersed to the depth of about 4 cm and was turned, manually, at the rate of about one turn per second on a circle, with radius of about 4 cm about the center of the jar. The signal was recorded several months before those described in Figs. 13 and 14, and is characterized by frequency content centered at 500 Hz.

In the report by Nori et al. [7], it is reported that  $f_d$  is in the range of 50 to 80 Hz during avalanches at Sand Mountain. The near equality of  $f_d$ , when the sand is "pulled" or pushed or sheared by the hand at the depth of about 10 cm and when the sand avalanches freely, merits special consideration. Namely, if the vibration is due to a boundary layer at the bottom of the fingers, then it could also be due to such a layer induced by the weight of the overburden, when the conditions exist for an avalanche to be triggered. Furthermore, if  $L_f < 0.1$ , then  $f_d = f_1$  is independent of  $M = SH\rho$ , where  $H$  is the depth of the boundary layer (8). Specifically, if  $H = 10$  cm,  $b = 5$  mm and  $c_s/c_p = 1/20$ , then  $L_f = 0.05$ . In such a scenario, the grains in the surface layers oscillate to the tune of the modes of vibration in the boundary layer, *i. e.*, the grain-grain collisions become synchronized. However,  $f_d$  is not determined by the time required for one grain to overtake another. The vibration in the boundary layer can give rise to surface waves propagating in the avalanching sand mass and in the sand bed ahead of the avalanche, as reported by Andreotti [20]. Furthermore, in the case of the avalanching dunes (Andreotti [20]) and in the case of the grains shaken in a jar (Leach and Rubin [11]), the weak decrease of  $f_d$  with increasing average diameter,  $\bar{d}$ , can be attributed to the weak increase of the thickness of the boundary layer and or the weak decrease of the shear phase velocity, with increasing  $\bar{d}$ .

However, it can also be argued that under the sliding plate there is a quasi-compacted sand band of well-defined thickness, for example 20 cm, with  $c_s \approx 40$  m/s, resulting in the frequency  $f_2 \approx 100$  Hz. Then, the modes of vibration would become excited by the sliding plate in the same sense the modes in a violin string become excited by the sliding bow chord. In such a scenario, the mechanism for the seismic and acoustic emissions is centered around the existence of a well-defined sand band and a substrate where  $c_s$  is much larger than 40 m/s. However, the observation described by Lewis [10] is not consistent with such a scenario. That is, when the dune sand mass was pushed uphill by the four fingers, the frequency of the acoustic emission was higher than when pushed downhill. In the context of this study, when the sand is pushed uphill, the stress level around the fingers is higher, resulting in a higher frequency. Similarly, in the case of the impacted grains in a dish, the higher pestle velocity results in a higher stress level around the pestle and in a higher frequency.

In the most recent report by Vriend et al. [22], the authors conclude that the seismic emission in an avalanching sand dune is due to a compression wave propagating in a band of dry sand, about 1.5 m in depth. The phase velocity in the sand band was determined to be 260 m/s and that in the air above and in the substrate was determined to be 356 and 310 m/s respectively, in a given case. They argue that for such phase velocities, a compression wave propagating downhill experiences total reflection at the upper and lower boundaries of the band as it bounces between the two boundaries, and thus, all the energy from the avalanching sand is converted to wave energy in the dry sand band. The spectrum from a booming dune, shown in the report by Nori et al. [7], is centered at about 85 Hz and has half width of about 6 Hz. Its overall appearance is similar to that of the main envelope shown in Figs. 4 and 5. Such a spectrum implies uniform thickness and well-defined boundaries of the dry sand band. However, the phase velocity of the avalanching sand mass, about 10 cm thick, is not likely to be equal to that in the stationary sand below and the band thickness is not likely to remain the same with distance downhill. Then, there is the question of the reflected waves at the top and the bottom of the hill. Furthermore, such an approach cannot account for the observations described above (Lewis [10] and Criswell et al. [24]), regarding the emissions when the sand mass is pushed by the hand. In the context of this study, the boundary layer plays the role of the violin string and the dry sand band below plays the role of the sound box.

## 2.5 Grains shaken in a jar

In order to investigate the possibility that layers near the surface, sliding over one another, are responsible for the acoustic emissions when musical grains are shaken in a jar, silica gel grains were placed in a glass jar, 6 cm in diameter by 10 cm in height, with the grain depth amounting to about 4 cm. The jar was shaken up-down along an axis about  $45^\circ$  from the vertical, the microphone being about 10 cm away. The signals, viewed on the oscilloscope screen, were characterized by a dominant frequency,  $f_d \approx 336 \pm 100$  Hz. Then, the same grains were placed in a plastic jar,  $4 \times 4$  cm in cross-section by 9 cm in height. The same procedure was followed, and the dominant frequency was,  $f_d \approx 463 \pm 100$  Hz. The assumption that the emitted sound originates with several grain layers sliding over one another leads to relative velocity between layers,  $V_r = 16$  cm/s, if  $\bar{d} = 0.4$  mm and  $f_d = 400$  Hz. This, in turn, leads to surface grain velocity equal to 1.6 m/s, if there are 10 sliding layers. This velocity is even higher since there is bound to be sliding at the jar wall. However, such high grain velocities are not present in the jars. Moreover, it will be argued in Section 2.6 that, in the context of the theory of sliding surface layers, the impact signal generated by a given grain as it overtakes the grains below, has to be nearly periodic. However, the lack of roundness and the large spread in the grain size (Fig. 2) nearly preclude such periodicity. Therefore, we have to seek the origin of the acoustic emission in the boundary layer at the wall of the jar, where the stress level is maximum. Furthermore, the dependence of  $f_d$  on the rigidity and surface texture of the jar wall is consistent with such a scenario.

In the plots of the period,  $T_d = 1/f_d$ , versus the number of grains,  $N$ , in a glass jar (Leach et al. [25]), we observe a weak increase of  $T_d$  with  $N$ , suggesting that  $L_f < 0.1$ , on the basis of Fig. 11, if  $f_d = f_1$ . When sand grains from Sand Mountain were shaken in a glass jar,  $f_d \approx 280$  Hz (Leach and Rubin [11]), while, when the same grains avalanched on the slip face of Sand Mountain,  $f_d \approx 66$  Hz (Nori et al. [7]). Such a difference in  $f_d$  can be attributed to the lower rigidity of the dune substrate relative to that of the jar wall, which results in a larger boundary layer thickness  $b$ . Similarly, when a glass jar is rapidly tilted or rotated about its axis along a horizontal direction (Lewis [10]), the origin of the acoustic emission can be sought in the boundary layer at the jar wall. There is a good analogy between the rapid tilting of the glass jar and the sudden opening of the gate controlling the height of the sand mass above the slip face on a sand dune (Douady et al. [21]).

In order for the acoustic emission to be evoked, the acceleration and deceleration of the jar must have substantial values. Effectively, a minimum amount of energy is required for the asperity fluidization to take place. Another observation supportive of the existence of a boundary layer at the jar wall, responsible for such emissions, can be found in the so called "frog sand cell". The cell, which was obtained from the Nima Sand Museum, in Nima, Japan, is an acrylic resin cylinder, 12 cm in length by 6 cm in diameter, sealed at both ends. It contains 100 ml of water and enough quartz sand so that, when its axis remains horizontal, the water level stands about 2 mm above the sand. When the cell is shaken back and forth, it emits a frog-like sound with  $f_d \approx 700$  Hz. Such signals can be seen in (Patitsas [9]). When the cell was rotated slowly about its axis so as no avalanches could be seen, a tactile sensation could be felt, however, no sound could be heard.

## 2.6 The harmony of the overtones and the periodicity of the impact waves

The scope of the inclusion of this Section is to establish that the harmonics, observed in the frequency spectra of the impacted singing grains, are not due to modes of vibration, but rather due to the periodic nature of the strings of the impact waves generated as the grains collide with the pestle. Since the depth of penetration amounted to less than 10 mm, it is safe to assume that the dominant frequency at 252 Hz, in Fig. 4, corresponds to the frequency  $f_2$  and that the frequency  $f_1$  was not excited due to insufficient stress level very near the surface. Furthermore, we can observe the presence of harmonics of  $f_2$  at 500 and 750 Hz. The radial particle displacement,  $\xi_r$ , corresponding to the frequency  $f_1$ , has a relatively large particle

displacement at the pestle boundary and decreases monotonically to zero at  $r = R + b$ . The expression for  $\xi_r$  is listed below Equation (17). The large amplitude of vibration at  $r = R$  implies that a relatively large amount of energy is required for it to become excited, since the amplitude of oscillation of the rod is also relatively large. This explains why the microphone detects this mode when the depth of penetration is larger and the stress level is higher, as can be seen in Figs. 8a and 14.

The radial particle displacement, for the mode with frequency  $f_2$ , resembles the first half of a sine function, where  $\xi_r = 0$  at  $r = R + b$ , but slightly less than zero at  $r = R$ . The grain mass oscillates in unison between the two boundaries, thus, drawing energy from the collisions between the pestle surface and the adjacent grains, as a violin string draws energy from the moving bow chord. It can be argued that most of the energy detected by the microphone originates directly from such interaction, and that can explain why the signal often becomes fainter with pestle depth, and why the geophone cannot detect such a signal (Figs. 13, 14 and 16). Effectively, we think that once the mode with frequency  $f_2$  is set in motion, the particle displacement is low, so as not to be detected by the geophone, but sufficiently large to result in the near synchronization of the collisions between the pestle and the adjacent grains. Then, the string of impact waves (pulses), generated by a given grain as it collides repeatedly with the descending pestle, is nearly periodic, the average time interval between impacts,  $\bar{T}$ , being equal to  $1/f_2$ . Such impact waves travel through the air to the site of the microphone and are invisible to the geophone. In the reports by Andreotti [20] and by Bonneau et al. [26], we encounter the somewhat similar concept, where the modes of vibration in the sand mass on a sand dune are thought to result in the "synchronization" of the collisions between the avalanching grains.

The amplitude of a given impact wave was defined as,  $\cos[(\pi/2)(q/T_j)t]$  in the interval,  $0 < t' < T_j/q$ , and as  $0.5\cos[(\pi/2)(q/T_j)t]$  in the interval,  $T_j/q < t < 3T_j/q$ , where,  $t' = t - t_j$ , where  $t_j$  is the time of the  $j^{th}$  collision in a given string, and  $T_j = t_{j+1} - t_j$ . The parameter  $q$  determines the time span of a given impact wave. The signal,  $\zeta_M(t)$ , generated by the string of  $M$  such impacts of a given grain with the pestle, is perfectly periodic if  $T_j = \text{constant} = T_d = 1/f_d$ . Furthermore, the superposition of  $N$  such signals, from  $N$  grains, is also perfectly periodic. The factor, 0.5, was included so that the net area under the curve is equal to 0. This, in turn minimizes the DC effect in the computation of the Fourier transform of the signal so synthesized. The square of the absolute value of the Fourier transform is identified as the Energy Density Spectrum, or the Frequency Spectrum, of the signal. Otherwise, the choice of the function representing the impact waves is not critical in the computation of the frequency spectrum. When  $T_j = \text{constant}$ , the frequency spectrum of the net signal comprises a bell shaped major envelope centered at  $f_d$  and minor envelopes centered at  $2f_d$ ,  $3f_d$ , etc. Furthermore, the height of the minor envelopes, relative to that of the major envelope, decreases with increasing  $q$ , i. e., with the duration of the impact waves. In the case of the Fraunhofer diffraction pattern by a set of  $M$  slits arranged along a line (Stone [27]), the relative height of the minor envelopes decreases with the width of the slits. When  $T_j$  vary randomly in the range  $T_d(1 \pm \Delta)$ , where  $\Delta = 0.08$ , secondary peaks appear adjacent to the various envelopes, and for  $q = 4.0$  and  $f_d = 252$  Hz, the spectrum of the synthesized signal resembles quite well the spectrum seen in Fig. 4. For larger values of  $\Delta$ , the envelopes are lost in the multitude of adjacent peaks and the spectrum resembles that of a noise-signal.

The secondary envelopes, at 500 and 750 Hz in Fig. 4, could be due to the excitation of the modes with frequencies  $f_3$  and  $f_4$ , and or, due to the near periodicity of the strings of the impact waves. The computation that leads to Fig. 12 reveals that the ratios  $f_3/f_2$  and  $f_4/f_2$  are equal to 1.62 and 2.24 when  $L_f = 0.001$ , 1.9 and 2.83 when  $L_f = 1.0$ , and 1.95 and 2.92 when  $L_f = 6.0$ . These results are consistent with (8), where the roots above the first occur at  $\alpha b = \pi, 2\pi, 3\pi$  etc as  $L_f \rightarrow \infty$ . Therefore, unless the pestle is overloaded, i. e.,  $L_f \rightarrow \infty$ , the minor envelopes cannot be due to the excitation of the modes with frequencies  $f_3, f_4$  etc. Such a dilemma has to be resolved by the proper experimental procedures, where the mass  $M$  and the velocity ratio  $c_s/c_p$  can be determined. The mode with frequency  $f_3$  has the same nodes at the boundaries as the mode with frequency  $f_2$  and a node at about

the middle. The excitation of such a mode is not consistent with the lack of cohesive forces between the grains and it is not likely to become excited, especially when the boundary layer thickness,  $b$ , is very small. The frequency spectrum, in Fig. 5, compared to that in Fig. 4, suggests that the higher velocity of penetration of the pestle resulted in a larger value of the parameter  $\Delta$ , described above, *i. e.*,  $\Delta$  was somewhat larger than 0.08. The sound associated with the signal in Fig. 5 was not as musical as that associated with the signal in Fig. 4. Such a reduction in musicality with the velocity of the pestle penetration was also recognized by Miwa et al. [3].

In the report by Nori et al. [7], we find the emission signal, having duration about 30 ms, from a so called "squeaking" sand. However, the depth of the sand bed and the type of the pestle used is not described. The frequency spectrum has a pronounced envelope at  $f_d = 860$  Hz and distinct secondary envelopes at multiples of  $f_d$ , *i. e.*, at 1720 and 2580 Hz. Similarly in the report by Takahara [1], the signal emitted, when Kotobikihama sand in a glass funnel was impacted by a rounded wood rod, has a frequency spectrum with dominant frequency,  $f_d = 599$  Hz, and four minor components at multiples of  $f_d$ . Evidently,  $f_d$  is equal to  $f_2$ . The mode corresponding to the highest frequency,  $f_6 = 5f_2$ , has four nodes in the interval,  $R < r < R + b$ , rendering its excitation highly unlikely. From the discussion that leads to (31.1) in the book by Landau and Lifshitz [18], it can be concluded that the fluid behaves more like a solid as the frequency of the wave motion increases, and thus, the phase velocity increases with frequency, *i. e.*, there is frequency dispersion. Therefore, the reason for the harmony in the frequency components has to be sought in the periodicity of the strings of the impact waves.

### 3. CONCLUSIONS

The study of the frequency spectra of the seismic and acoustic emissions, from a bed of musical grains impacted by a pestle, is an effective approach towards the understanding of the mechanism responsible for such emissions. There is experimental evidence that when the grain bed is impacted by a pestle, the relatively high rigidity in a bed of musical grains results in shear bands or slip channels, where presumably the modulus of rigidity approaches zero. However, such slip channels cannot account for the observed acoustic emissions. The overall continuity of the acoustic signals, during the pestle penetration into the grain bed, leads to the conclusion that the source of such emissions has to be sought in a relatively thin grain boundary layer at the bottom of the pestle. Such a layer, only a few mm thick, has very low modulus of rigidity and thus very low shear phase velocity. The grains in the boundary layer remain in close contact as they slide past one another. In this sense, the determining factor for musicality is the physical state of the grain asperities, while grain shape and roundness are nearly irrelevant. The high stress level in the boundary layer results in the liquidization of the grain asperities at the contact points and this in turn results in the drastic reduction in the modulus of rigidity. Alternatively, this effect could be due to the formation, at the grain contact points, of sub-micron colloidal particles, which act as ball bearings between two hard surfaces.

The theoretical frequency spectrum, corresponding to the modes of vibration in such a layer, is nearly independent of the geometry of the bottom of the pestle, in agreement with experimental observations. The spectrum comprises a relatively low frequency,  $f_1$ , and a series of frequencies,  $f_2, f_3, f_4 \dots$ , where  $f_3, f_4 \dots$  are somewhat lower than the multiples of  $f_2$ . The mode of vibration corresponding to the frequency,  $f_1$ , resembles that of a thin elastic rod fixed at one end and loaded with the mass,  $M$ , at the other end. As  $M \rightarrow \infty$ , the mode of vibration resembles that of a short weightless spring loaded with the mass  $M$ , thus,  $f_1$  decreases as  $M^{-0.5}$ .

In the present study, the signals with frequency,  $f_1$ , were recorded more reliably using a geophone, while the signals with the higher frequency,  $f_2$ , were recorded more reliably using a microphone. Furthermore, the signals recorded by the geophone were nearly sinusoidal

and not characterized by the usual higher frequency components, as in the signals recorded by the microphone. The reason for such difference can be found in the fundamentally different processes in generating the signals. That is, whereas, in the case of the frequency,  $f_1$ , the signals are generated by the usual up-down motion of the pestle, in the case of the frequency,  $f_2$ , the signals are generated predominately by the superposition of the different quasi-periodic strings of the impact waves generated by the grains, as they collide with the descending pestle.

Grains can be classified as singing or musical, if a pleasant sound is emitted when they are placed in a large dish, to a depth of several cm, and impacted lightly by a rod about 2 cm in diameter. The hissing sound emitted by a bed of ordinary (silent) grains, when impacted by a pestle, has frequency content extending up to several thousand Hz. In the context of this study, the upper end of the frequency content is due, primarily, to the incoherent grain-grain collisions in the neighborhood of the pestle, not unlike the collision process in an assembly of molecules in the gaseous state. Furthermore, the lower end of the frequency content is attributable to modes of vibration in a diffuse and ill-defined boundary layer around the impacting bottom of the pestle. Even the silent grains become somewhat musical when squeezed in a confined geometry, in particular, when impacted by a pestle in a cup to the depth of only about 1 cm. Effectively, the rigidity of the cup floor results in the formation of a boundary layer, albeit a not so well-defined layer.

The origin of the acoustic emissions when jars, about half filled with musical grains, are rapidly tilted or shaken along their axis, can be sought in the boundary layer at the jar wall. Furthermore, the concept of the boundary layer, at the bottom of an avalanching sand bed on the face of a dune, can provide another way of looking at the nearly 150 year old mystery and controversy surrounding the seismic and acoustic emissions from booming dunes. In the context of this study, the boundary layer plays the role of the violin string and the dry sand band below, reported to be about 1.5 m thick, plays the role of the sound box. The relatively low frequencies characterizing the emissions from sand avalanches, compared to those when the same sand is shaken in a jar, can be justified in terms of the relatively low rigidity of the sand mass below the avalanching grains. Effectively, the lower rigidity of the stationary sand mass below the avalanching grains results in a thicker boundary layer. It is conceivable that such a boundary layer could contribute to the sound emitted during a snow avalanche.

Hopefully, this study will serve to stimulate further investigation into the mechanism responsible for such seismic and acoustic emissions. In particular, more experimental results are needed in order to establish directly the existence of the boundary layer and the reasons for the precipitous decrease in the modulus of rigidity in the boundary layer, when the musical grains are impacted or squeezed. What is the physical state of the grain surface that is responsible for such a decrease?

## APPENDIX. Wave motion

### A<sub>1</sub>. Wave propagation

Firstly, we attempt to establish that the observed frequency spectra cannot originate with waves propagating in a semi-infinite interval, since in such a case the frequencies have to be defined by some parameter(s), which does not exist when the pestle penetrates into the grain bed. In particular, if there were wave propagation away from the pestle, it would propagate along the slip channels and or along the surface of the pestle towards the surface. For the sake of simplicity, we assume that the pestle, in Fig. 3, is wide enough so that there is no variation of the particle displacement with,  $z$ , and that a wave propagates along the surface of the pestle along  $-\hat{x}$  on the  $xz$  plane. In particular, we assume that the boundary layer, of thickness  $b$ , extends all along the pestle surface, and that it serves as a conduit, where the energy generated at the bottom of the pestle is transported upwards. We consider only the layer on the right side of the pestle and we assume that  $y = 0$  on the pestle surface. The bottom front end of the pestle is ignored for the sake of this argument. Furthermore, in what follows we assume that the fluid is non-viscous in order not to have to deal with complex phase velocities. Then, we write,

$$\Psi = [A_1 \cos \gamma y + B_1 \sin \gamma y] e^{j(kx + \omega t)}, \quad A_z = [A_2 \cos \beta y + B_2 \sin \beta y] e^{j(kx + \omega t)}, \quad (1)$$

where the scalar  $\Psi$  represents the compression or dilatational wave and  $A_z$  is the component along  $\hat{z}$  of the vector  $\mathbf{A}$  representing the shear wave.  $\Psi(x, y)$  satisfies the scalar wave equation with phase velocities  $c_p$ , and  $\mathbf{A}(x, y)$  satisfies the vector wave equation with phase velocity  $c_s$  (Graff [28]). These bulk phase velocities are expressed as,

$$c_p = \sqrt{\frac{\lambda_e + 2\mu}{\rho}}, \quad c_s = \sqrt{\frac{\mu}{\rho}}, \quad (2)$$

where  $\lambda_e, \mu$  are the Lamé constants and  $\rho$  is the mass density. In particular,  $\mu$  is the shear modulus or the modulus of rigidity. The wave number  $k$  satisfies the following equations,

$$k = \omega/c, \quad k_p = \omega/c_p, \quad k_s = \omega/c_s, \quad k^2 = k_p^2 - \gamma^2, \quad k^2 = k_s^2 - \beta^2, \quad (3)$$

where  $c_s < c_p$ . The particle displacement, which is also the grain displacement due to the compression wave can be written as,

$$\xi_p = \nabla \Psi = \hat{x}(jk)[A_1 \cos \gamma y + B_1 \sin \gamma y] + \hat{y}(\gamma)[-A_1 \sin \gamma y + B_1 \cos \gamma y], \quad (4)$$

and that due to the shear wave as,

$$\xi_s = \nabla \times \mathbf{A} = \hat{x}(\beta)[-A_2 \sin \beta y + B_2 \cos \beta y] + \hat{y}(-jk)[A_2 \cos \beta y + B_2 \sin \beta y], \quad (5)$$

where the factor  $e^{j(kx + \omega t)}$  is understood to be included. According to the grain contact fluidization hypothesis, the grain mass outside the boundary layer remains in a quasi-solid state, whereas, the grain mass in the boundary layer is in a viscoelastic-liquid state, where  $c_p \gg c_s$ . From the boundary condition,  $\xi_{py} = 0$  at  $y = 0$ , we conclude that  $A_1 = 0$ , and from the condition,  $\xi_{py} = 0$  at  $y = b$ , we conclude that  $\gamma = \pi/b = 500\pi$ , if  $b = 2$  mm. From the propagation condition,  $k = \omega/c$ ,  $k_p = \omega/c_p$ ,  $k^2 = k_p^2 - \gamma^2$ , we conclude that for propagation to occur,  $k_p$  has to be larger than  $\gamma$ , and that implies that  $c_p$  has to be smaller than  $\omega/\gamma = f_d/250 = 1.8$  m/s, if  $f_d = 450$  Hz. However, according to our hypothesis,  $c_p$  is on the order of hundreds of m/s. Therefore, we need consider only shear wave propagation. Then, the above arguments are applicable with  $B_2, \beta, k_s, c_s$  in place of  $B_1, \gamma, k_p, c_p$ , in (4). Thus, we can write,  $\beta b = n\pi$ ,  $n = 1, 2, 3$ , which defines the cut-off frequencies,  $\omega_n = n\pi c_s/b$ . These cut-off frequencies are the eigenfrequencies in the case of the standing wave patterns. Thus, when wave propagation is in effect, the angular frequencies  $\omega$  cannot be specified by the physical parameters,  $c_s$  and  $b$  alone. Effectively, the frequencies have to be specified by

a parameter outside the boundary layer and the only such parameter is the velocity of the descending pestle. However, when a wood rod, 16 mm in diameter by 123 cm in length, was allowed to free-fall on the silica gel grains in the 9 cm diameter glass jar, the average frequency of the acoustic emission increased from 420 Hz to 500 Hz, while the drop height increased from about 2 cm to 15 cm. That is, while the impact velocity increased by the factor of 2.7, the frequency increased only by 17%. In general, when the pestle was driven into the grain bed with more force and more velocity, the increase in the frequency was moderate. In the report by Nishiyama and Mori [3], it is stated that the frequency of the signal, emitted from a bed of singing sand, increased by about 20% as the mean penetration velocity of the rod increased from 7 to 35 cm/s. Furthermore, on page 43 in the report by Lewis [11], we read that, a plank, 45 cm long by 5 cm wide and 1.25 cm thick, was used to push the sand mass on a dune surface with various velocities  $V$ . It was then estimated, using a series of tuning pitch pipes, that when  $V$  was about 15 cm/s,  $f_d$  was about 100 Hz (low C), while when  $V$  was about four times as large,  $f_d$  was about twice as large.

### A<sub>2</sub>. Flat rectangular bottom

For the sake of simplicity, we assume that the pestle has a flat bottom and that the boundary layer, on the  $yz$  plane in Fig. 3, has uniform thickness,  $b$ , and extends from  $y = 0$  to  $y = 2R$  along the surface of the pestle and  $R \gg b$ . The length of the pestle along  $\hat{z}$ ,  $L$ , is assumed to be considerably larger than  $R$ . Again, we write,

$$A_z = [A_1 \cos \alpha x + B_1 \sin \alpha x][A_2 \cos \beta y + B_2 \sin \beta y] \quad (6)$$

where  $k_s^2 = \alpha^2 + \beta^2$ . The expressions for the particle displacements are,  $\xi_x = [A_1 \cos \alpha x + B_1 \sin \alpha x] \beta [-A_2 \sin \beta y + B_2 \cos \beta y]$ , and  $\xi_y = \alpha [A_1 \sin \alpha x - B_1 \cos \alpha x][A_2 \cos \beta y + B_2 \sin \beta y]$ . From the condition,  $\xi_x = 0$  at  $x = b$ , it follows that  $B_1 = -A_1 \cot \alpha b$ . The normal stress along  $\hat{x}$  is,  $\sigma_{xx} = (\lambda_e + 2\mu) \partial \xi_x / \partial x \approx \lambda_e \partial \xi_x / \partial x$ , since  $\mu \ll \lambda_e$ . Furthermore, at  $x = 0$  we can write,

$$\sigma_{xx} S = M \frac{\partial^2 \xi_x}{\partial t^2} = -M \omega^2 \xi_x \quad (7)$$

Then, the following transcendental equation can be derived,

$$\cot(\alpha b) = \frac{M}{\rho S b} \left( \frac{c_s}{c_p} \right)^2 (\alpha b) = L_f(\alpha b) \quad (8)$$

where  $L_f$ , the load factor, is the slope of the straight line,  $S$  is the surface of the bottom of the pestle, *i. e.*,  $S = 2LR$ ,  $M$  is the mass of the pestle, and  $k_s \approx \alpha$  since  $\beta \ll \alpha$ , since  $R \gg b$ . It is the familiar equation that gives the frequencies of vibration of an elastic thin rod, fixed at one end and loaded with the mass,  $M$ , at the other end. The first root,  $\alpha_1 b$ , corresponding to the vibration of a loaded short spring, lies in the interval,  $0 < \alpha b < \pi/2$ , the second root lies in the interval,  $\pi < \alpha b < 3/2\pi$  and so on. When  $M(c_s/c_p)^2$  is sufficiently large so that  $\alpha_1 b \rightarrow 0$ ,  $\cot(\alpha b) \rightarrow 1/\alpha b$ , and the first root varies as  $1/\sqrt{M}$ . Such a variation of the frequency of the emission with the mass of the pestle can be seen in the report by Nishiyama and Mori [3].

### A<sub>3</sub>. Rounded cylindrical bottom

In this section, we consider the same pestle, *i. e.*, wide enough along the  $z$  axis so that there is no variation with  $z$ , but rounded to a circular end at the bottom, as depicted in Fig. 3. The boundary layer has thickness  $b$  and outer radius  $R_1 = R + b$  and is limited nearly to the bottom of the pestle, where the stress level is maximum. We proceed to write in cylindrical coordinates,  $\mathbf{A} = A_z(r, \theta) \hat{z} e^{j(\omega t)}$ , where

$$\nabla^2 \mathbf{A} = \nabla(\nabla \cdot \mathbf{A}) - \nabla \times \nabla \times \mathbf{A} = \frac{1}{c_s^2} \frac{\partial^2 \mathbf{A}}{\partial t^2} \quad (9)$$

It is straight forward process to show that,  $\nabla \cdot \mathbf{A} = 0$ , and that,

$$\nabla^2 \mathbf{A} = -\hat{z} \left[ -\frac{1}{r} \frac{\partial A_z}{\partial r} - \frac{\partial^2 A_z}{\partial r^2} - \frac{1}{r^2} \frac{\partial^2 A_z}{\partial \theta^2} \right] = -k_s^2 A_z \hat{z} \quad (10)$$

The above equation is the Bessel differential equation and the solutions can be written in the form of (VI.4) in the book by Stratton [29] i. e.,

$$A_z = A_n f_1(\theta) f_2(r) e^{j(\omega t)} \quad (11)$$

where,  $f_1(\theta)$  is  $\cos(n\theta)$  or  $\sin(n\theta)$ , and  $f_2(r)$  is one of the ordinary Bessel functions,  $J_n(r)$  of the first kind or  $Y_n(r)$  of the second kind. The particle displacement is,

$$\xi = \nabla \times \mathbf{A} = \hat{r} \frac{1}{r} \frac{\partial A_z}{\partial \theta} - \hat{\theta} \frac{\partial A_z}{\partial r} \quad (12)$$

The index,  $n = 0$ , results in the unrealistic mode where the radial displacement,  $\xi_r = 0$ , and values of  $n$  greater than 1 result in modes with nodal points in the boundary layer. We tend to think that such modes cannot become excited in a boundary layer, only about 5mm thick, due to lack of cohesive forces between the grains and also due to lack of roundness and due to a large size distribution of the grains. We choose  $-\sin\theta$  rather than  $\cos\theta$  so that we can write the more suitable expressions,

$$\xi_r = -\frac{1}{r} \cos\theta [A_1 J_1(kr) + Y_1(kr)], \quad \xi_\theta = k \sin\theta [A_1 J_1'(kr) + B_1 Y_1'(kr)] \quad (13)$$

As in the previous section, we write,  $2RL\lambda_e\sigma_{rr} = M\partial^2\xi/\partial t^2$  at the surface of the pestle and we arrive at the equation,

$$[(1 - L_f \zeta^2) J_1(\zeta) - \zeta J_1'(\zeta)] A_1 + [(1 - L_f \zeta^2) Y_1(\zeta) - \zeta Y_1'(\zeta)] B_1 = 0 \quad (14)$$

where the load factor is written as,  $L_f = M/(\rho 2LR^2)(c_s/c_p)^2$  where  $L$  is the length of the pestle along the  $z$  axis, and  $\zeta = kR$ . In the above derivation, the contribution from the tangential stress,  $\sigma_{r\theta} = \mu(1/r \partial \xi_r / \partial r + \partial \xi_\theta / \partial r - \xi_\theta / r)$ , was neglected since  $\mu \ll \lambda_e$ . Furthermore, we assume that at  $r = R + b = R_1$ ,  $\xi_r = 0$ , resulting in the equation,

$$J_1(\zeta \chi) A_1 + Y_1(\zeta \chi) B_1 = 0 \quad (15)$$

where,  $\chi = 1 + b/R$ . Equations (14, 15) take the place of (8) in seeking the roots for  $k$  and  $\omega$  for given  $L_f, R, b$ , and  $c_s$ .

#### A.4. Rounded spherical bottom

In Fig. 3, the  $z$  axis takes the place of the  $x$  axis, and the  $x$  axis is into the plane of the paper. Thus, the angle  $\theta$ , in Fig. 3, becomes the azimuthal angle  $\phi$ . We proceed to write in spherical polar coordinates,

$$\mathbf{A} = \hat{\theta} A_\theta(r, \phi) e^{j(\omega t)} \quad (16)$$

Furthermore, due to the symmetry about the  $z$  axis, we restrict the variation with  $r$  and  $\phi$  on the  $yz$  plane where  $\theta = \pi/2$ . Then, it follows that  $\nabla \cdot \mathbf{A} = 0$ , and also the components of  $\nabla \times \nabla \times \mathbf{A}$  along  $\hat{r}$  and  $\hat{\phi}$  are equal to 0, and we arrive at an equation similar to (VII.3) in the book by Stratton [29], namely,

$$r^2 \frac{\partial^2 A_\theta}{\partial r^2} + 2r \frac{\partial A_\theta}{\partial r} + \frac{\partial^2 A_\theta}{\partial \phi^2} = -r^2 k^2 A_\theta \quad (17)$$

As in the previous section, we choose to write,  $A_\theta = -\sin\phi[A_1j_1(kr) + B_1y_1(kr)]$ , and then,  $\xi_r = 1/r\cos\phi[A_1j_1(kr) + B_1y_1(kr)]$ , and  $\xi_\phi = -1/r\cos\phi[A_1j_1(kr) + B_1y_1(kr)] - k\cos\phi[A_1j_1'(kr) + B_1y_1'(kr)]$ , where  $j_1(kr)$  and  $y_1(kr)$  are the spherical Bessel functions of the first and second kind. Next, we write again at  $r = R$ ,  $\sigma_{rr}\pi R^2 = M\partial^2\xi_r/\partial t^2$ , and we arrive at (14, 15) above with  $2L$  replaced by  $\pi R$ , and  $J_1(kR)$ ,  $Y_1(kR)$  replaced by  $j_1(kR)$ ,  $y_1(kR)$ , i. e., the load factor is written as,

$$L_f = \frac{M}{\rho\pi R^3} \left(\frac{c_s}{c_p}\right)^2 \quad (18)$$

### A<sub>5</sub>. Flat circular bottom

As in the previous section, the  $z$  axis points straight down in Fig. 3, and the  $x$  axis points into the plane of the paper. The boundary layer has the form of a disk of radius  $R$  and thickness  $b$ , at the bottom of the pestle. We write in cylindrical coordinates,

$$\mathbf{A} = \hat{\theta}A_\theta(r, z)e^{i(\omega t)} \quad (19)$$

Then, from the component of  $\nabla(\nabla \cdot \mathbf{A}) - \nabla \times \nabla \times \mathbf{A}$  along  $\hat{r}$ , we obtain the equation,

$$\frac{\partial^2 A_\theta}{\partial r^2} + \frac{1}{r} \frac{\partial A_\theta}{\partial r} - \frac{1}{r^2} A_\theta + \frac{\partial^2 A_\theta}{\partial z^2} = -k_s^2 A_\theta \quad (20)$$

This is an unfamiliar differential equation, however, its solution,  $f_1(r)$ , is of no importance in the context of this study. Thus,

$$\xi_z = \frac{1}{r} \frac{\partial}{\partial r} (r f_1) [A_1 \cos \alpha z + B_1 \sin \alpha z] \quad (21)$$

Then, as in section A<sub>2</sub>, we obtain (8) with  $S = \pi R^2$ .

### References

- Takahara, H. (1973). Sounding mechanism of singing sand. *Journal of the Acoustical Society of America*, 53, 634-639.
- Nishiyama, K. & Mori, S. (1982). Frequency of sound from singing sand. *Japanese Journal of Applied physics*, 21, 591-595.
- Miwa, S., Hidaka, J. & Shimosaka, A. (1983). Musical sand. *Powder Science and Technology in Japan, KONA*, 1, 64-72.
- Haff, P. K. (1986). Booming dunes. *American Scientist*, 74, 376-381.
- Qu, J., Sun, B., Zhang, W., Wang, Y. & Kang, G. (1995). Surface texture of quartz grain in booming sand and its acoustic significance. *Chinese Science Bulletin*, 40, 1719-1723.
- Sholtz, P., Bretz, M. & Nori, F. (1997). Sound-producing sand avalanches. *Contemporary Physics*, 38, 329-342.
- Nori, F., Sholtz, P. & Bretz, M. (1997). Booming sand. *Scientific American* 277, 84-89.
- Brown, A. W., Campbell, W. A., Jones, J. M. & Thomas, E. R. (1964).

Musical sand: The singing sands of the seashore part II. *Proc. Univ. Newcastle Upon Tyne Philos. Soc.*, 1, 1-21.

Patitsas, A. J. (2003). Booming and singing acoustic emissions from fluidized granular beds. *Journal of Fluids and Structures*, 17, 287-315.

Lewis, A. W. (1936). Roaring sands of the Kalahari Desert. *South African Geographical Journal*, 19, 33-50.

Leach, M. F. & Rubin, A. G. (1990). The acoustics of booming sand. *Progress in Acoustic Emission V, Proceedings of the 10th International Acoustic Emission Symposium, The Japanese Society for Non-destructive Inspection, Japan*, 239-244.

- Grambo, R. (2006). Dune Tunes. *Canadian Geographic*, January/February.
- Courzon, M. (1923). *Tales of Travel*, p. 292. Hodder and Stoughton.
- Bolton, H. C. (1889). Researches on sonorous sand in the Peninsula of Sinai. *Proceedings of the American Association for the Advancement of Science*, 38, 137-159.
- Bagnold, R. A. (1941). *The Physics of Blown Sand and Desert Dunes*, 247-257. London, Chapman and Hall.
- Goldsack, D. E., Leach, M. F. & Kilkenny, C. (1997). Natural and artificial singing sands. *Nature*, 386, 29.
- Kilkenny, C., Leach, M. F. & Goldsack, D. E. (1997). The acoustic emission of silica gel. *Canadian Acoustics*, 25, 28.
- Landau, L. D. & Lifshitz, E. M. (1959). *Theory of Elasticity*, p. 130. Reading Mass., Addison-Wesley.
- Joseph, D. D. (1990). *Fluid Dynamics of Viscoelastic Liquids*, p. 565. New York, Springer-Verlag.
- Andreotti, B. (2004). The song of dunes as a wave-particle mode locking. *Physical Review Letters*, 93, 238001-1-4.
- Douady, S., Manning, A., Hersen, P., Elbelrhiti, H., Protiere, S., Daerr, A. & Kabbachi, B. (2006). Song of dunes as a self-synchronized instrument. *Physical Review Letters*, 97, 018002-1-4.
- Vriend, N. M., Hunt, M. L., Clayton, R. W., Brennen, C. E., Brantley, K. S. & Ruiz-Angulo, A. (2007). Solving the mystery of the booming dunes. *Geophysical Research Letters*, 34, L16306.
- Humphries, D. W. (1966). The booming sand of Corizo, Sahara, and the squeaking sand of Gower, S. Wales. *Sedimentology*, 6, 135-152.
- Criswell, D. R., Lindsay, J. F. & Reasoner, D. L. (1975). Seismic and acoustic emissions of a booming dune. *Journal of Geophysical Research*, 80, 4963-4974.
- Leach, M. F., Goldsack, D. E. & Kilkenny, C. (1999). Booming sand as a possible source of single frequency sound. *Proceedings of the Sixth International Congress on Sound and Vibration, 1983-1988*. Copenhagen, Denmark.
- Bonneau, L., Andreotti, B. & Clement, E. (2007). Surface elastic waves in granular media under gravity and their relation to booming avalanches. *Physical Review E*, 75, 016602.
- Stone, J. M. (1963). *Radiation and Optics*, p. 143. New York, McGraw-Hill Book Company.
- Graff, K. F. (1975). *Wave Motion in Elastic Solids*. Columbus Ohio, Ohio State University Press.
- Stratton, J. A. (1941). *Electromagnetic Theory*. New York, McGraw-Hill.